Pergamon

Int. J. Solids Structures Vol. 32, No. 20, pp. 2945–2960, 1995

0020–7683/95 $9.50 + .00

0020–7683(94)00270–3

FREE VIBRATION OF PIEZOELECTRIC LAMINATES IN CYLINDRICAL BENDING

PAUL HEYLIGER and STEPHEN BROOKS
Department of Civil Engineering, Colorado State University, Fort Collins, CO 80523, U.S.A.

(*Received* 20 *July* 1994; *in revised form* 14 *November* 1994)

Abstract—Exact solutions are presented for the free vibration behavior of piezoelectric laminates in cylindrical bending. The laminates can be composed of an arbitrary number of elastic and piezoelectric layers. The natural frequencies and through-thickness modal distributions are computed for the case where the upper and lower surfaces of the laminate are traction free. The electrostatic potential or the normal electric displacement is specified to be zero at these surfaces. All appropriate interface conditions are also satisfied. The resulting determinant equation is iteratively solved for the resonant frequencies, with the mode distributions of the elastic and electric field variables also computed. Representative examples are studied for thick and thin laminate geometries.

1. INTRODUCTION

The free vibration of elastic laminates has been studied in detail by Jones (1969, 1971) for the case of cylindrical bending and by Srinivas *et al.* (1970) and Srinivas and Rao (1970) for finite rectangular plates. Studies of the exact vibration behavior of laminates containing piezoelectric layers have seen limited investigation. The work of Tiersten (1969) provided the theoretical foundations and numerous examples of the dynamic behavior of piezoelectric plates, but most of the geometries studied therein were composed of single layers.

In this study, the coupled dynamic equations of linear piezoelectricity are solved for laminates composed in whole or in part by piezoelectric layers under the conditions of cylindrical bending and periodic motion. No kinematic assumptions are used to describe the behavior of the electric and elastic field variables. The equations of motion, the charge equation, and the boundary and interface conditions are satisfied exactly. The methodology and results presented here are expected to provide the necessary means with which to compare more versatile and efficient approximate techniques for the analysis of finite piezoelectric laminates under more general conditions.

2. METHODOLOGY

Geometry and governing equations

A laminate composed either completely or in part of piezoelectric layers is shown in Fig. 1. The x axis is out-of-plane, with the y and z axes corresponding to the respective axial and transverse coordinates of the laminate. The laminate is assumed to be infinitely long in the x-direction, with perfect bonding between layers. A bond-line may be simulated using a layer of small thickness. The laminate is of length L, the total thickness is h, and

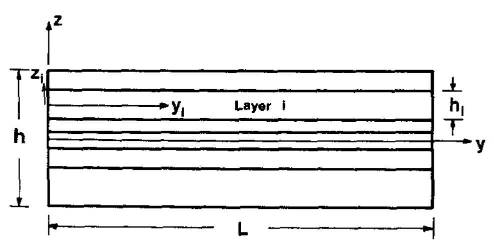

Fig. 1. Geometry of the laminate in cylindrical bending.

the i-th layer has thickness h_i. Layer 1 is the top layer of the laminate and layer n is the bottom layer. In the ensuing discussion, the use of a local thickness coordinate is used for each layer. This originates at the left end of the horizontal centerline of each layer.

Each of the n layers has the constitutive relations

$$\begin{aligned} \sigma_i &= C_{ij}S_j - e_{ki}E_k \\ D_k &= e_{kj}S_j + \varepsilon_{km}E_m, \end{aligned} \tag{1}$$

where $i, j = 1, 2, \ldots, 6$ and $k, m = 1, 2, 3$. Here σ_i are the components of the stress tensor, C_{ij} are the elastic stiffness components, S_j are the components of infinitesimal strain, e_{ki} are the piezoelectric coefficients, E_k are the components of the electric field, D_k are the components of the electric displacement, and ε_{km} are the dielectric constants. The poling direction for the piezoelectric laminate is coincident with the x_3 or z axis.

The displacement components u_i are related to the strain components through the relations

$$S_{ij} = \frac{1}{2}\left(\frac{\partial u_i}{\partial x_j} + \frac{\partial u_j}{\partial x_i}\right). \tag{2}$$

Here the conventional notation for the strain indices has been used to be consistent with eqn (1), i.e. $S_{11} = S_1$, $2S_{23} = S_4$, etc., and $x_1 = x$, $x_2 = y$ and $x_3 = z$. Under the conditions of cylindrical bending, the displacement field takes the form $u_1 = u = 0$, $u_2 = v(y, z)$ and $u_3 = w(y, z)$, and the electrostatic potential has the form $\phi = \phi(y, z)$. Hence all variables are independent of the x coordinate, and terms containing a gradient in the x-direction vanish. The electric field components can be related to the electrostatic potential ϕ using the relation

$$E_i = -\frac{\partial \phi}{\partial x_i}. \tag{3}$$

As implied above, this yields $E_x = 0$.

The materials used in this study are assumed orthotropic, and have their principal material directions coincident with the x or y coordinate directions. The non-zero elastic stiffnesses used here are C_{22}, C_{23}, C_{33}, and C_{44}. The independent piezoelectric coefficients are e_{32}, e_{33}, and e_{24}, and the dielectric constants are ε_{22} and ε_{33}.

The equations of motion for each of the layers are given by

$$\begin{aligned} \frac{\partial \sigma_y}{\partial y} + \frac{\partial \tau_{yz}}{\partial z} &= \rho \frac{\partial^2 v}{\partial t^2} \\ \frac{\partial \tau_{yz}}{\partial y} + \frac{\partial \sigma_z}{\partial z} &= \rho \frac{\partial^2 w}{\partial t^2}. \end{aligned} \tag{4}$$

Here ρ denotes material density for a given layer and t is time.

Finally, the charge equation of electrostatics is given as

$$\frac{\partial D_y}{\partial y} + \frac{\partial D_z}{\partial z} = 0. \tag{5}$$

Substituting eqns (1)–(3) into eqns (4) and (5) gives the governing equations of the problem in terms of the displacement components v and w and the electrostatic potential ϕ as

$$C_{22}\frac{\partial^2 v}{\partial y^2}+C_{23}\frac{\partial^2 w}{\partial y\,\partial z}+e_{32}\frac{\partial^2 \phi}{\partial y\,\partial z}+C_{44}\left(\frac{\partial^2 v}{\partial z^2}+\frac{\partial^2 w}{\partial y\,\partial z}\right)+e_{24}\frac{\partial^2 \phi}{\partial y\,\partial z}=\rho\frac{\partial^2 v}{\partial t^2} \tag{6}$$

$$C_{33}\frac{\partial^2 w}{\partial z^2}+C_{23}\frac{\partial^2 v}{\partial y\,\partial z}+e_{24}\frac{\partial^2 \phi}{\partial y^2}+C_{44}\left(\frac{\partial^2 w}{\partial y^2}+\frac{\partial^2 v}{\partial y\,\partial z}\right)+e_{33}\frac{\partial^2 \phi}{\partial z^2}=\rho\frac{\partial^2 w}{\partial t^2} \tag{7}$$

$$e_{33}\frac{\partial^2 w}{\partial z^2}+e_{32}\frac{\partial^2 v}{\partial y\,\partial z}-\varepsilon_{22}\frac{\partial^2 \phi}{\partial y^2}+e_{24}\left(\frac{\partial^2 w}{\partial y^2}+\frac{\partial^2 v}{\partial y\,\partial z}\right)-\varepsilon_{33}\frac{\partial^2 \phi}{\partial z^2}=0. \tag{8}$$

Each of these equations must be satisfied for the material properties of a specific layer. In addition to these equations, the boundary conditions on the upper surface of layer 1 and the bottom surface of layer n must be specified. For the study of free vibration, these two surfaces are assumed to be traction free, which can be stated as

$$\sigma_z\left(y,\frac{h_1}{2}\right)=0 \tag{9}$$

$$\sigma_z\left(y,-\frac{h_n}{2}\right)=0 \tag{10}$$

$$\tau_{yz}\left(y,\frac{h_1}{2}\right)=0 \tag{11}$$

$$\tau_{yz}\left(y,-\frac{h_n}{2}\right)=0. \tag{12}$$

Here it is assumed that the spatial dependence of each field quantity is written in terms of the axial variable y and the local thickness variable. Rather than index the latter variable, it is denoted simply as z with the understanding that it refers to an individual layer coordinate and not that of the total laminate.

In addition to the mechanical boundary conditions, the electric surface conditions must be satisfied. This is accomplished in this study by specifying either homogeneous electrostatic potential or normal electric displacement. The homogeneous potential represents a grounded surface electrode, while a zero normal electric displacement is indicative of a charge-free surface. The conditions on the electric field variables are denoted as

$$\phi\left(y,\frac{h_1}{2}\right)=0 \text{ or } D_z\left(y,\frac{h_1}{2}\right)=0, \text{ and either } \phi\left(y,-\frac{h_n}{2}\right)=0 \text{ or } D_z\left(y,-\frac{h_n}{2}\right)=0.$$

Exact solution

In cylindrical bending, the laminate is simply supported and the vertical edges are assumed to be grounded. These conditions are expressed as

$$\sigma_y(0,z)=\sigma_y(L,z)=0 \tag{13}$$

$$w(0,z)=w(L,z)=0 \tag{14}$$

$$\phi(0,z)=\phi(L,z)=0. \tag{15}$$

At each interface between layers, continuity conditions of displacement, traction, potential, and normal electric displacement must be enforced. As with the solution of

Pagano (1969, 1970), an indexing scheme is used to express the conditions for the i-th layer as

$$\sigma_z^i\left(y,\frac{-h_i}{2}\right)=\sigma_z^{i+1}\left(y,\frac{h_{i+1}}{2}\right) \tag{16}$$

$$\tau_{yz}^i\left(y,\frac{-h_i}{2}\right)=\tau_{yz}^{i+1}\left(y,\frac{h_{i+1}}{2}\right) \tag{17}$$

$$v^i\left(y,\frac{-h_i}{2}\right)=v^{i+1}\left(y,\frac{h_{i+1}}{2}\right) \tag{18}$$

$$w^i\left(y,\frac{-h_i}{2}\right)=w^{i+1}\left(y,\frac{h_{i+1}}{2}\right) \tag{19}$$

$$\phi^i\left(y,\frac{-h_i}{2}\right)=\phi^{i+1}\left(y,\frac{h_{i+1}}{2}\right) \tag{20}$$

$$D_z^i\left(y,\frac{-h_i}{2}\right)=D_z^{i+1}\left(y,\frac{h_{i+1}}{2}\right). \tag{21}$$

Here i represents the layer number and h_i is the thickness of the i-th layer. At each interface of a laminate with n plies, there are four conditions related to the elastic variables and two conditions related to the electric variables for a total of $6(n-1)$ conditions. At the top and bottom surfaces, there are two elastic boundary conditions and one electric condition for a total of six conditions. Enforcing all conditions leads to $6n$ equations relating the variables within all layers of the laminate.

The conditions in eqns (13)–(15) are satisfied identically using solutions of the form

$$\begin{aligned}(v,w,\phi)&=(V(z)\cos py,\ W(z)\sin py,\ \phi(z)\sin py)\\&=(\hat{U}\cos py,\ \hat{W}\sin py,\ \hat{\phi}\sin py)\exp(sz)\exp(\mathrm{j}\omega t).\end{aligned} \tag{22}$$

Here the $\hat{}$ symbol denotes a constant, z is the local thickness coordinate of the lamina, s is an unknown quantity, $\mathrm{j}=\sqrt{-1}$, and ω is the natural frequency of vibration. Substitution of these expressions into the equilibrium and charge equations results in the system of equations

$$\begin{bmatrix} C_{44}s^2-C_{22}p^2+\rho\omega^2 & ps(C_{23}+C_{44}) & ps(e_{32}+e_{24}) \\ -ps(C_{44}+C_{23}) & C_{33}s^2-C_{44}p^2+\rho\omega^2 & e_{33}s^2-e_{24}p^2 \\ -ps(e_{24}+e_{32}) & e_{33}s^2-e_{24}p^2 & \varepsilon_{22}p^2-\varepsilon_{33}s^2 \end{bmatrix}\begin{Bmatrix}\hat{V}\\ \hat{W}\\ \hat{\phi}\end{Bmatrix}=\begin{Bmatrix}0\\0\\0\end{Bmatrix}. \tag{23}$$

Setting the determinant of this matrix to zero for a non-trivial solution yields the characteristic equation

$$-As^6+Bs^4+Cs^2+D=0, \tag{24}$$

where the constants A, B, C, and D are given as

$$A=C_{44}C_{33}\varepsilon_{33}+C_{44}e_{33}^2 \tag{25}$$

$$\begin{aligned}B=&(C_{22}C_{33}\varepsilon_{33}-2C_{23}e_{24}e_{33}-2C_{23}e_{32}e_{33}-C_{23}^2\varepsilon_{33}-2C_{23}C_{44}\varepsilon_{33}-2C_{44}e_{32}e_{33}+C_{44}C_{33}\varepsilon_{22}\\&+e_{24}^2C_{33}+C_{22}e_{33}^2+2e_{32}e_{24}C_{33}+e_{32}^2C_{33})p^2+(-\rho C_{33}\varepsilon_{33}-C_{44}\rho\varepsilon_{33}-\rho e_{33}^2)\omega^2\end{aligned} \tag{26}$$

$$C = (-C_{22}C_{44}\varepsilon_{33} - C_{22}C_{33}\varepsilon_{22} + 2C_{23}e_{32}e_{24} - 2C_{22}e_{33}e_{24} + C_{23}^2\varepsilon_{22} + 2C_{23}C_{44}\varepsilon_{22} - e_{32}^2C_{44} + 2C_{23}e_{24}^2)p^4 + (C_{22}\rho\varepsilon_{33} + C_{44}\rho\varepsilon_{33} + 2\rho e_{33}e_{24} + \rho C_{33}\varepsilon_{22} + e_{32}^2\rho + C_{44}\rho\varepsilon_{22} + 2e_{32}e_{24}\rho + e_{24}^2\rho)\omega^2p^2 - \rho^2\omega^4\varepsilon_{33} \quad (27)$$

$$D = (C_{22}C_{44}\varepsilon_{22} + C_{22}e_{24}^2)p^6 + (-C_{22}\rho\varepsilon_{22} - e_{24}^2\rho - C_{44}\rho\varepsilon_{22})\omega^2p^4 + \rho^2\omega^4\varepsilon_{22}p^2. \quad (28)$$

The sixth-order characteristic equation (24) can be expressed as the third-order equation

$$g^3 + dg + f = 0. \quad (29)$$

The nature of the subsequent solution for each layer of the laminate depends on the roots g. There can be three real and distinct roots, three real roots, at least two of which are equal, and the case where there is one real root and two conjugate complex roots. The case of repeated roots was not found for any of the materials considered in this study. Only the remaining two cases are considered.

Case 1 : *real roots for* g

Given three real roots for g, the roots of the original sixth-order equation can be determined by considering

$$\gamma = s^2 = g + \frac{B}{3A}. \quad (30)$$

This will lead to six roots for m, which are either real or imaginary depending on the sign of γ. Following the nomenclature of Pagano (1969), the solution for the displacement and electrostatic potential components can be written in either case as

$$V(z) = \sum_{j=1}^{3} V_j(z) \quad W(z) = \sum_{j=1}^{3} L_jW_j(z) \quad \phi(z) = \sum_{j=1}^{3} R_jW_j(z), \quad (31)$$

where

$$V_j = F_jC_j(z) + G_jS_j(z)$$
$$W_j = G_jC_j(z) + \alpha_jF_jS_j(z). \quad (32)$$

Here F_j and G_j are constants, $j = 1, 2, 3$, and the functions C and S and the parameter m are defined as

$$C_j = \cosh(m_jz) \quad S_j(z) = \sinh(m_jz) \quad \alpha_j = 1 \quad (\gamma > 0) \quad (33)$$

$$C_j = \cos(m_jz) \quad S_j(z) = \sin(m_jz) \quad \alpha_j = -1 \quad (\gamma < 0) \quad (34)$$

$$m_j = \left|g_j + \frac{B}{3A}\right|^{1/2}. \quad (35)$$

The values for the coefficients in eqn (31) are given by

$$L_j = \frac{pm_j}{J_j}[(\alpha_jm_j^2\varepsilon_{33} - p^2\varepsilon_{22})(C_{23} + C_{44}) + (\alpha_jm_j^2e_{33} - e_{24}p^2)(e_{24} + e_{32})] \quad (36)$$

$$R_j = \frac{pm_j}{J_j}[(\alpha_j m_j^2 e_{33} - e_{24}p^2)(C_{44}+C_{23}) + (C_{44}p^2 - \rho\omega^2 - \alpha_j m_j^2 C_{33})(e_{24}+e_{32})] \quad (37)$$

$$J_j = (\alpha_j m_j^2 \varepsilon_{33} - p^2\varepsilon_{22})(\alpha_j m_j^2 C_{33} + \rho\omega^2 - p^2 C_{44}) + m_j^4 e_{33}^2 - 2\alpha_j m_j^2 p^2 e_{33} e_{24} + e_{24}^2 p^4. \quad (38)$$

Using the constitutive relations in eqn (1) allows the components of stress and electric displacement to be given by

$$\sigma_i = \sin py \sum_{j=1}^{3} (-pC_{2i} + \alpha_j m_j L_j C_{i3} + \alpha_j m_j R_j e_{3i}) V_j(z) \quad (39)$$

$$\tau_{yz} = \cos py \sum_{j=1}^{3} (C_{44} m_j + C_{44} p L_j + e_{24} p R_j) W_j(z) \quad (40)$$

$$D_y = \cos py \sum_{j=1}^{3} (m_j + pL_j - \varepsilon_{22} p R_j) W_j(z) \quad (41)$$

$$D_z = \sin py \sum_{j=1}^{3} (-pe_{32} + e_{33}\alpha_j m_j L_j - \varepsilon_{33}\alpha_j m_j R_j) V_j(z). \quad (42)$$

Here the expression for the normal stresses implies σ_1, σ_2 and σ_3 are equal to σ_x, σ_y and σ_z, respectively.

If the layer is not piezoelectric, the equations above no longer hold because the electric and elastic fields uncouple. With the exception of the inertial term influence, the elastic fields are identical in nature to those determined by Pagano (1969). They are shown here in a different form. The roots m_1–m_4 corresponding to the elastic solution are those of the characteristic equation

$$C_{44}C_{33}m^4 + (2C_{23}C_{44} - C_{22}C_{33} + C_{23}^2)p^2 m^2 + C_{22}C_{44}p^4 + \rho^2\omega^4 = 0 \quad (43)$$

and the roots corresponding to the electrostatic solution are given by

$$n_{1,2} = \pm p\sqrt{\frac{\varepsilon_{22}}{\varepsilon_{33}}}. \quad (44)$$

The displacement components and electrostatic potential are given by

$$V(z) = \cos py \sum_{j=1}^{4} A_j \exp(m_j z) \quad (45)$$

$$W(z) = \sin py \sum_{j=1}^{4} A_j \alpha_j \exp(m_j z) \quad (46)$$

$$\phi(z) = \sin py \sum_{j=1}^{2} B_j \exp(n_j z). \quad (47)$$

Here A_j and B_j are constants, the values for m_j are now the roots of eqn (43), and

$$\alpha_j = \frac{pm_j(C_{44}+C_{23})}{(C_{33}m_j^2 - C_{44}p^2 + \rho\omega^2)}. \quad (48)$$

The components of stress and electric displacement are given by

$$\sigma_i = \sin py \sum_{j=1}^{4} (C_{i3}\alpha_j m_j - C_{2i}p)A_j \exp(m_j z) \tag{49}$$

$$\tau_{yz} = \cos py \sum_{j=1}^{4} (m_j + p\alpha_j)A_j \exp(m_j z) \tag{50}$$

$$D_y = -\varepsilon_{22} p \cos py \sum_{j=1}^{2} B_j \exp(n_j z) \tag{51}$$

$$D_z = -\varepsilon_{33} \sin py \sum_{j=1}^{2} B_j n_j \exp(n_j z). \tag{52}$$

Case 2: complex roots for g

For some material and geometry combinations, there will be one real root for g and two roots that are complex conjugate. The case of real roots for g has been discussed in the previous section, and the focus here is on the remaining two roots. When γ in eqn (30) is complex, the two complex conjugate roots of g can be used to express the final four roots of m as $\pm(a \pm ib)$, where $i = \sqrt{-1}$ and a and b are positive constants. The general solution for V in this case can be expressed as

$$V(z) = k_1\, e^{(a+ib)z} + k_2\, e^{(a-ib)z} + k_3\, e^{(-a+ib)z} + k_4\, e^{(-a-ib)z}, \tag{53}$$

where k_1–k_4 are complex constants. This can be expressed in terms of real functions as

$$V(z) = e^{az}(c_1 \cos bz + c_2 \sin bz) + e^{-az}(c_3 \cos bz + c_4 \sin bz), \tag{54}$$

where c_1–c_4 are now real constants. Using eqn (23), the corresponding solution for W can be written as

$$\begin{aligned} W(z) = {} & e^{az}\{[\Gamma_1(ac_1+bc_2)+\Omega_1(ac_2-bc_1)]\cos bz \\ & +[\Gamma_1(ac_2-bc_1)-\Omega_1(ac_1+bc_2)]\sin bz\} + e^{-az}\{[\Gamma_1(bc_4-ac_3)+\Omega_1(ac_4+bc_3)]\cos bz \\ & +[\Gamma_1(-ac_4-bc_3)+\Omega_1(bc_4-ac_3)]\sin bz\}. \end{aligned} \tag{55}$$

Here the parameters Γ_1 and Ω_1 are defined to be

$$\Gamma_1 = \frac{\xi_1\xi_3 + \xi_2\xi_4}{\xi_3^2 + \xi_4^2} \tag{56}$$

$$\Omega_1 = \frac{\xi_2\xi_3 - \xi_1\xi_4}{\xi_3^2 + \xi_4^2}, \tag{57}$$

where $\xi_1 = \mathscr{R}(pF_1)$, $\xi_2 = \mathscr{F}(pF_1)$, $\xi_3 = \mathscr{R}(pF_2)$, $\xi_4 = \mathscr{F}(pF_2)$, with the functions F_1 and F_2 given by

$$F_1 = [\varepsilon_{33}(a^2-b^2+2iab)-\varepsilon_{22}p^2](C_{44}+C_{23})+[e_{33}(a^2-b^2+2iab)-e_{24}p^2](e_{24}+e_{32}) \tag{58}$$

$$F_2 = (e_{33}^2 + C_{33}\varepsilon_{33})[(a^2-b^2)^2 - 4a^2b^2 + 4\mathrm{i}ab(a^2-b^2)] + p^2(a^2-b^2+2\mathrm{i}ab)$$
$$\times\left(-C_{33}\varepsilon_{22} + \frac{\rho}{p^2}\omega^2\varepsilon_{33} - C_{44}\varepsilon_{33} - 2e_{33}e_{24}\right) + p^4(C_{44}\varepsilon_{22} + e_{24}^2) - \rho\omega^2\varepsilon_{22}p^2. \quad (59)$$

If the parameters β_1 and β_2 are introduced such that

$$\beta_1 = a\Gamma_1 - b\Omega_1 \quad \beta_2 = b\Gamma_1 + a\Omega_1, \quad (60)$$

then the solution for W can be cast in the final form

$$W(z) = \mathrm{e}^{az}[(c_1\beta_1 + c_2\beta_2)\cos bz + (-c_1\beta_2 + c_2\beta_1)\sin bz]$$
$$+ \mathrm{e}^{-az}[(-c_3\beta_1 + c_4\beta_2)\cos bz + (-c_3\beta_2 - c_4\beta_1)\sin bz]. \quad (61)$$

Using similar steps, the final solution for ϕ can be written as

$$\phi(z) = \mathrm{e}^{az}[(c_1\beta_3 + c_2\beta_4)\cos bz + (-c_1\beta_4 + c_2\beta_3)\sin bz]$$
$$+ \mathrm{e}^{-az}[(-c_3\beta_3 + c_4\beta_4)\cos bz + (-c_3\beta_4 - c_4\beta_3)\sin bz], \quad (62)$$

where in this case

$$\beta_3 = a\Gamma_2 - b\Omega_2 \quad \beta_4 = b\Gamma_2 + a\Omega_2. \quad (63)$$

Here the parameters Γ_2 and Ω_2 are defined to be

$$\Gamma_2 = \frac{\eta_1\xi_3 + \eta_2\xi_4}{\xi_3^2 + \xi_4^2} \quad (64)$$

$$\Omega_2 = \frac{\eta_2\xi_3 - \eta_1\xi_4}{\xi_3^2 + \xi_4^2}, \quad (65)$$

where $\eta_1 = \mathscr{R}(pF_3)$ and $\eta_2 = \mathscr{F}(pF_3)$, with

$$F_3 = [e_{33}(a^2-b^2+2\mathrm{i}ab) - e_{24}p^2](C_{44} + C_{23})$$
$$+ [-C_{33}(a^2-b^2+2\mathrm{i}ab) + C_{44}p^2 - \rho\omega^2](e_{24} + e_{32}). \quad (66)$$

The components for stress and electric displacement can be computed using the constitutive relations in eqn (1). These are lengthy but straightforward to construct and are not listed here.

The solutions given in this section correspond only to the complex conjugate roots. There will be an additional contribution to the solution through the appearance of the real root for g. These must be combined to form the complete solution for the layer.

Solution for the laminate

Solutions for the displacement components v and w, the electrostatic potential ϕ, the three non-zero stress components σ_y, σ_z, and τ_{yz}, and the two non-zero electric displacement components D_y and D_z are expressed in terms of six unknown constants for each of the n layers. This yields $6n$ total unknowns for the complete laminate. These constants are evaluated by enforcing the boundary and interface continuity conditions at the upper and lower surface of each layer within the laminate. There are three boundary conditions at the top of layer 1 and the bottom of layer n, with one from each of the pairs (v, τ_{yz}), (w, σ_z), and (ϕ, D_z) for a total of six boundary conditions. At each interface the continuity conditions as expressed in eqns (16)–(21) are enforced, leading to $6(n\text{-}1)$ equations. Hence the total number of equations and unknowns is $6n$. This can be expressed in matrix form as

$$[A]\{\delta\} = \{0\}. \tag{67}$$

Here the vector $\{\delta\}$ represents the unknown constants, with the entries in $[A]$ representing the values of their coefficients in the general solution.

For the free vibration problem, the coefficients A_{ij} are unknown since they are dependent on the unknown natural frequency ω. The additional constraint on this system to determine ω is the requirement for a non-trivial solution that $\det(A) = 0$. To find the values for the frequencies that enforce this condition, the frequency was stepped through a sequence of small increments and the sign of the determinant computed. Evaluating this parameter as a function of frequency yields regions near a zero determinant. After a sufficient number of sign crossings have been identified, the values for ω that yield a zero determinant can be isolated and refined using bisection. The sign change was monitored by computing the eigenvalues of $[A]$ using the QR algorithm in extended precision.

3. NUMERICAL EXAMPLES

Four examples are considered in this section: a single piezoelectric layer, a two-ply laminate of dissimilar piezoelectric materials, a symmetric three-ply hybrid laminate of piezoelectric and elastic layers, and a three-layer cross-ply of orthotropic piezoelectric material. All laminates are composed of materials termed A, B, C, and D. Materials A and B simulate piezoceramics (Berlincourt *et al.*, 1964), and possess transversely isotropic material properties. Materials C and D are orthotropic, with D being piezoelectric (Tashiro *et al.*, 1981). The properties for each of these materials are given in Table 1. For simplicity, the density of all four materials was set equal to 1.

The computational strategy and presentation of results is similar for each of the four examples. Only the first axial mode [$p = \pi/L$ in eqn (22)] is considered. For this mode, there are an infinite number of thickness modes that are possible. The first ten of these are documented here. For each laminate, two aspect (L/h) ratios of 4 and 50 are studied to represent a thick and thin plate. Also for each laminate, the top and bottom surfaces are either grounded at zero potential or the electric displacement is specified to zero. These two cases are termed closed and open conditions, respectively.

Results are given in terms of natural frequencies in radians per second. For the last three examples, representative through-thickness distributions of the elastic and electric field variables are also shown for the closed condition only. These have been normalized by dividing through by the maximum value for each field variable. The scaling factors are

Table 1. Elastic, piezoelectric, and dielectric properties of materials

Property	A	B	C	D
C_{11} (GPa)	81.3	136.	132.38	237.
C_{22}	81.3	136.	10.756	23.2
C_{33}	64.5	116.	10.756	10.5
C_{12}	0.329	0.204	0.24	0.154
C_{13}	0.432	0.201	0.24	0.178
C_{23}	0.432	0.201	0.49	0.177
C_{44}	25.6	55.2	3.606	2.15
C_{55}	25.6	55.2	5.6537	4.40
C_{66}	30.6	56.5	5.6537	6.43
e_{24} (C/m^2)	12.72	12.29	0	−0.01
e_{31}	−5.20	−5.35	0	−0.13
e_{32}	−5.20	−5.35	0	−0.14
e_{33}	15.08	15.78	0	−0.28
$\varepsilon_{33}/\varepsilon_0$	1300	1700	3.0	11.98
$\varepsilon_{11}/\varepsilon_0$	1475	1730	3.5	12.5

Table 2. Scale factors used in modal eigenfunction plots

Case	v	w	ϕ	σ_y	σ_z	τ_{yz}	D_z
[A/B]: $L/h = 4$	1.2273	3.44908	275318528	—	—	—	—
[A/B]: $L/h = 50$	0.79425	23.5538	12860534	—	—	—	—
[A/C/A]: $L/h = 4$	0.64500	2.99522	46113904	—	—	—	—
[A/C/A]: $L/h = 50$	0.47742	15.2998	2985087	—	—	—	—
[D(90/0/90)]: $L/h = 4$	2.64563	22.24023	104116752	0.123416e15	0.36794e12	0.97833e13	12.616
[D(90/0/90)]: $L/h = 50$	1.32676	43.3436	13970391	0.49517e13	0.23950e9	0.59835e11	0.59587e-2

shown for the three examples in Table 2, and should be multiplied by the corresponding distributions in each figure to obtain the final (unscaled) eigenfunctions.

Single piezoelectric layer

A single layer of material A is considered first. The thickness of the plate is 0.01 m. The resulting frequencies are shown in Table 3. These results indicate that the closed conditions generate lower frequencies than do the open case values, and this effect on the lower thickness modes is reduced as the plate becomes thin.

Two-layer laminate

A two-ply laminate is constructed of dissimilar piezoelectric materials with the lamination scheme [A/B]. Both layers are of equal thickness and the total thickness is 0.01 m. The resulting frequencies are given in Table 4.

Table 3. Frequencies $\omega/100$ for single layer of material A

	$L/h = 4$		$L/h = 50$	
Mode	Closed	Open	Closed	Open
1	52580.67	53046.76	373.6468	373.6770
2	234514.7	254503.6	18970.19	20614.86
3	560241.7	642210.4	503061.9	585842.0
4	969921.1	972665.4	1004822	1004959
5	1154042	1224774	1083123	1155798
6	1513042	1545515	1507996	1540083
7	2016798	2021621	2010659	2010691
8	2319013	2321388	2310478	2310496
9	2522449	2545884	2513332	2532907
10	3017998	3019775	3015942	3015954

Table 4. Frequencies $\omega/100$ for two-layer [A/B] laminate

	$L/h = 4$		$L/h = 50$	
Mode	Closed	Open	Closed	Open
1	56492.87	57056.04	398.0712	399.5398
2	272572.3	275664.7	22037.71	22199.65
3	642549.6	717847.4	578761.6	656277.1
4	1078116	1129993	1119205	1209600
5	1302643	1371236	1230936	1231074
6	1765606	1773905	1758431	1766933
7	2383141	2414676	2377974	2419966
8	2426698	2457413	2416459	2435533
9	2992976	3023384	2984263	3012504
10	3556566	3562834	3573218	3577041

The distributions of the two displacement components v and w are shown in Fig. 2a,b, with the corresponding through-thickness distribution of potential given in Fig. 2c. In this and all other figures, the solid line corresponds to the case $L/h = 4$, with the dashed line used for $L/h = 50$. The distribution for v is effectively a straight line for the thin plate, with a slight kink appearing at the interface for the thick plate along with a slightly pronounced non-linear behavior. The lower stiffness of the top plate is evident in both the relative magnitudes of the displacement v and also for w. The thin plate yields a distribution of transverse displacement that is nearly uniform, with a much larger difference for the thick plate. There is little variation in the potential for the two cases, with the break in slope at mid-plane appearing because of the change in material properties.

Hybrid elastic/piezoelectric laminate

Two layers of material A are bonded to the top and bottom of the non-piezoelectric material C. The thickness of each A layer is 0.001 m with the total laminate thickness 0.01 m. The frequencies are given in Table 5. The through-thickness distributions for v, w, and ϕ are shown in Fig. 3a–c. As expected, the behavior is symmetric about the mid-line for this geometry, with the stronger variations in the displacements appearing for the thick plate.

Three-layer cross-ply

A three-layer laminate is composed of material D with the orientation [90/0/90]. The outer two plies are 0.001 m thick, with the inner single layer at 0.002 m. The frequencies for this laminate are given in Table 6. The through-thickness distributions for v, ϕ, σ_y, σ_z, τ_{yz}, and D_z are shown in Fig. 4a–f, respectively. The plot for the transverse displacement w is not shown because for both aspect ratios the distribution is essentially constant through the thickness.

Table 5. Frequencies for three-layer [A/C/A] hybrid laminate

	$L/h = 4$		$L/h = 50$	
Mode	Closed	Open	Closed	Open
1	4061328.8	4061731.4	39410.624	39410.667
2	27900191	27901969	2247302.1	2247317.1
3	36428990	36443066	23844186	23852156
4	37712838	37714304	37843597	37843597
5	55899720	55958795	48150971	48156904
6	74615082	74681734	73373346	73526447
7	80757823	80850840	76831789	76832551
8	102701050	102981673	99514068	99545214
9	118100120	118104818	117398034	117398080
10	129070007	129537579	126327777	126790968

Table 6. Frequencies for three-layer [D(90/0/90)] laminate

	$L/h = 4$		$L/h = 50$	
Mode	Closed	Open	Closed	Open
1	8566377	8567554	128750.6	128751.3
2	57005399	57009902	5665109	5666352
3	82327042	84435642	38771456	38776573
4	89589873	89590675	81551011	83188177
5	113129345	113140575	83497176	84122248
6	144984544	144984646	131859172	131860373
7	168046083	168199382	167795156	167796226
8	186632764	186634205	175962338	175962356
9	224987615	224990384	213529592	213530684
10	250544158	251255053	250927913	251638468

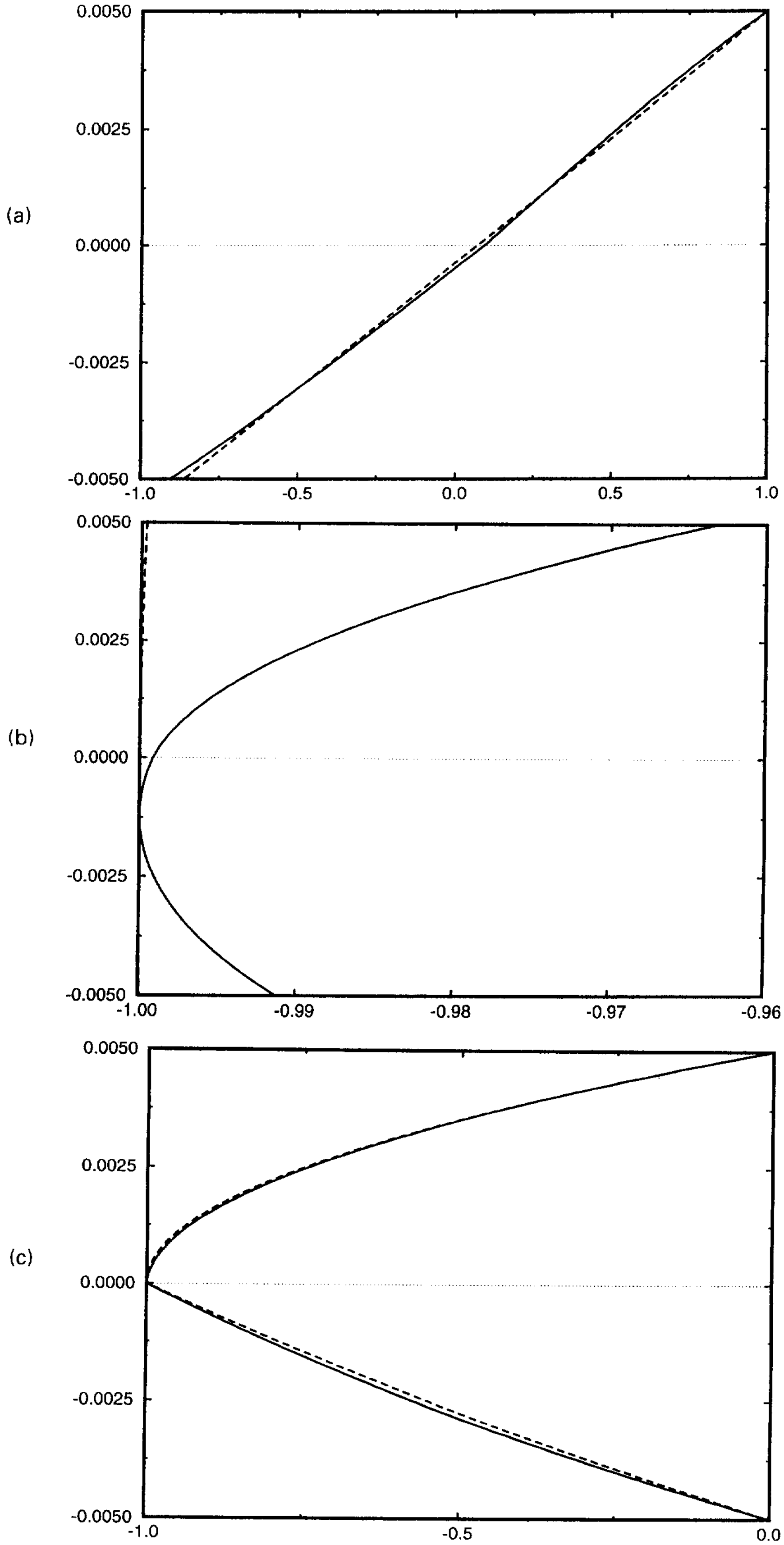

Fig. 2. Through-thickness mode shapes for two-layer laminate. (a) Axial displacement v. (b) Transverse displacement w. (c) Electrostatic potential ϕ.

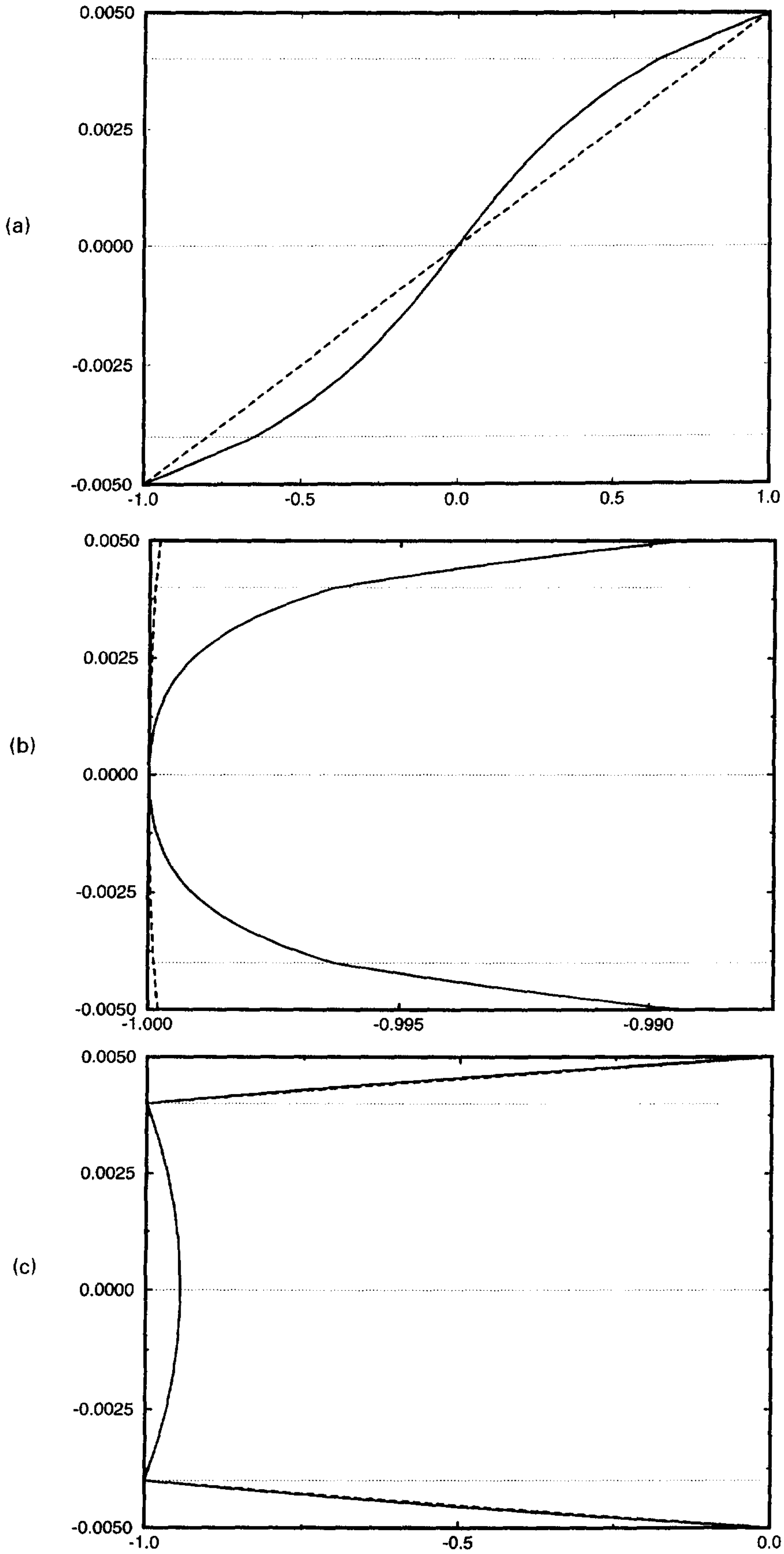

Fig. 3. Through-thickness mode shapes for three-layer hybrid laminate. (a) Axial displacement v. (b) Transverse displacement w. (c) Electrostatic potential ϕ.

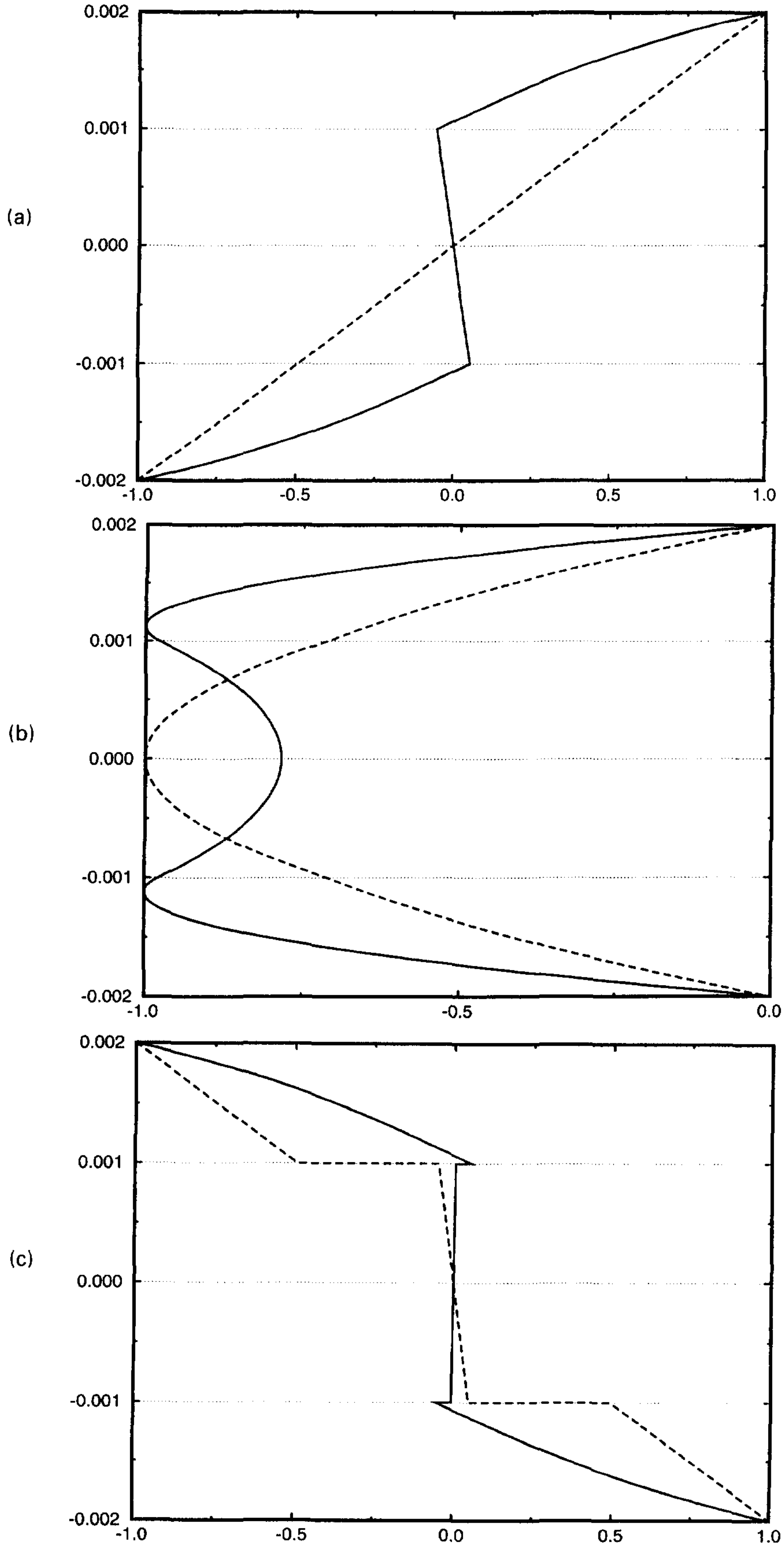

Fig. 4. Through-thickness mode shapes for three-layer cross-ply. (a) Axial displacement v. (b) Electrostastic potential ϕ. (c) Axial normal stress σ_y. (d) Transverse normal stress σ_z. (e) Transverse shear stress τ_{yz}. (f) Transverse electric displacement D_z.

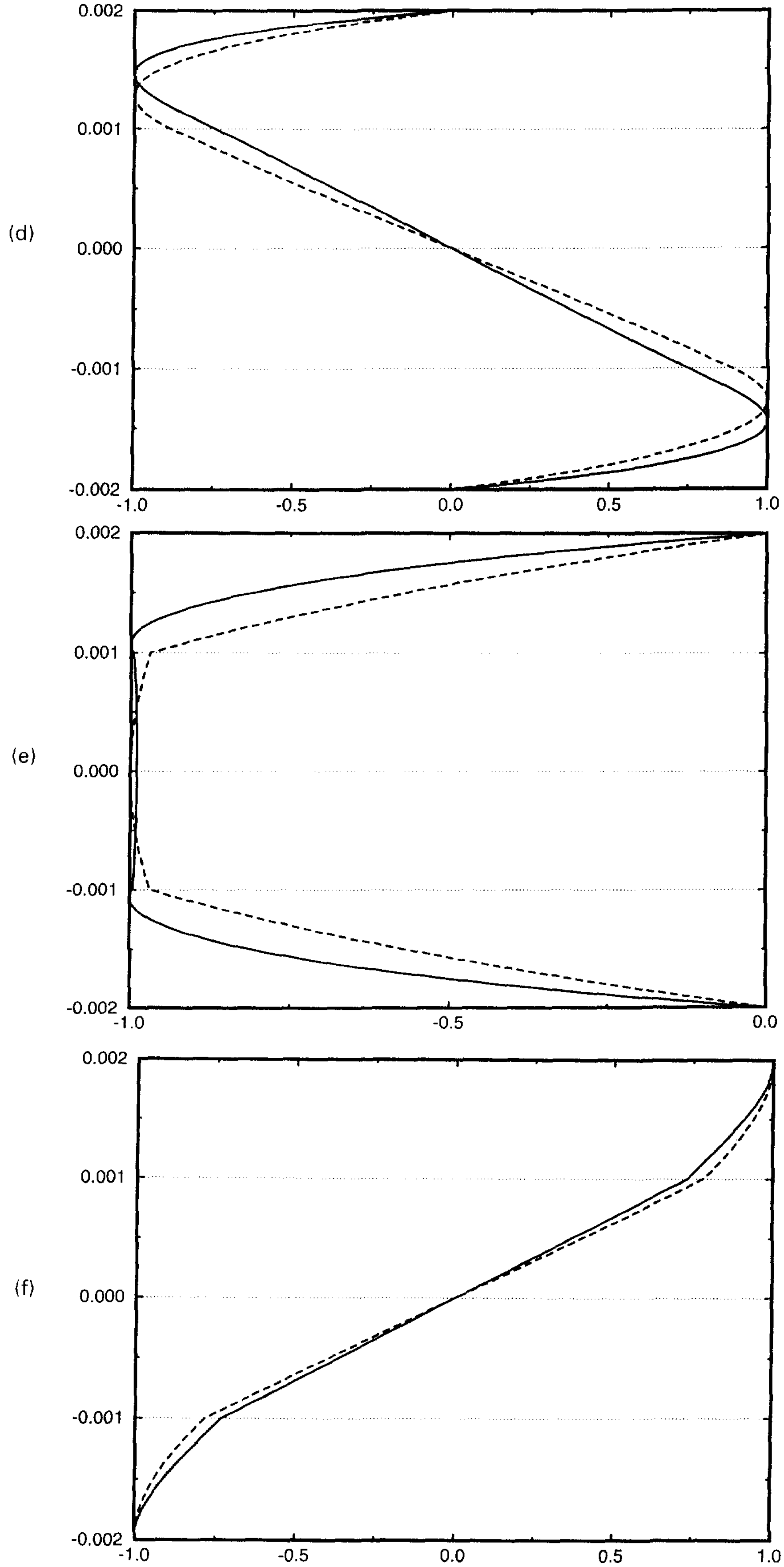

Fig. 4. *Continued.*

4. CONCLUSIONS

The closed condition on the horizontal faces of the laminate consistently results in lower natural frequencies regardless of aspect ratio or piezoelectric strength. This effect is reduced as the aspect ratio of the plate is increased. For materials with smaller piezoelectric coefficients, the influence of the electric boundary conditions is lessened.

The nature of the displacement and potential distributions through the thickness of the laminate indicates that, for thick plates especially, simple plate theories may not represent the true field behavior. The axial displacement and the electrostatic potential distributions in particular are not represented well using a simple linear approximation. This is true for the fundamental modes studied here and becomes even more evident for the higher thickness modes. The development of piezoelectric plate theories may benefit from assumed kinematic and potential behavior that represents at least the lower modes of free vibration to a sufficient degree.

REFERENCES

Berlincourt, D. A., Curran, D. R. and Jaffe, H. (1964). Piezoelectric and piezomagnetic materials and their function in transducers. In *Physical Acoustics* (Edited by W. P. Mason), Vol. 1, pp. 169–270. Academic Press, New York.

Jones, A. T. (1969). Exact natural frequencies for cross-ply laminates. *J. Compos. Mater.* **4,** 476–491.

Jones, A. T. (1971). Exact natural frequencies and modal functions for a thick off-axis lamina. *J. Compos. Mater.* **5,** 504–520.

Pagano, N. J. (1969). Exact solutions for composites in cylindrical bending. *J. Compos. Mater.* **3,** 398–411.

Pagano, N. J. (1970). Exact solutions for rectangular bidirectional composites and sandwich plates. *J. Compos. Mater.* **4,** 20–34.

Srinivas, S., Rao, C. V. J. and Rao, A. K. (1970). Some results from an exact analysis of thick laminates in vibration and buckling. *J. Appl. Mech.* **37,** 868–870.

Srinivas, S. and Rao, A. K. (1970). Bending, vibration and buckling of simply supported thick orthotropic rectangular plates and laminates. *Int. J. Solids Structures* **6,** 1463–1481.

Tashiro, K., Tadokoro, H. and Kobayashi, M. (1981). Structure and piezoelectricity of poly(vinylidene fluoride). *Ferroelectrics* **32,** 167–175.

Tiersten, H. F. (1969). *Linear Piezoelectric Plate Vibrations.* Plenum Press, New York.